HHS Public Access

Author manuscript

Magn Reson Med. Author manuscript; available in PMC 2023 March 21.

Published in final edited form as:

Magn Reson Med. 2008 August ; 60(2): 258–264. doi:10.1002/mrm.21616.

Ischemia-Induced Changes of Intracellular Water Diffusion in Rat Glioma Cell Cultures

Theodore P. Trouard[1,2,*], **Kevin D. Harkins**[1], **Joseph L. Divijak**[2], **Robert J. Gillies**[1,2,3], **Jean-Philippe Galons**[2]

[1]Biomedical Engineering Program, University of Arizona, Tucson, Arizona, USA.

[2]Department of Radiology, University of Arizona, Tucson, Arizona, USA.

[3]Arizona Cancer Center, University of Arizona, Tucson, Arizona, USA.

Abstract

Diffusion-weighted MRI is commonly used in the diagnosis and evaluation of ischemic stroke because of the rapid decrease observed in the apparent diffusion coefficient (ADC) of tissue water following ischemia. Although this observation has been clinically useful for many years, the biophysical mechanisms underlying the reduction of tissue ADC are still unknown. To help elucidate these mechanisms, we have employed a novel three-dimensional (3D) hollow-fiber bioreactor (HFBR) perfused cell culture system that enables cells to be grown to high density and studied via MRI and MRS. By infusing contrast media into the HFBR, signals from intracellular water and extracellular water are spectroscopically resolved and can be investigated individually. Diffusion measurements carried out on C6 glioma HFBR cell cultures indicate that ischemia-induced cellular swelling results in an increase in the ADC of intracellular water from 0.35 $\mu m^2/ms$ to approximately 0.5 $\mu m^2/ms$ (diffusion time = 25 ms).

Keywords

diffusion; MRI; MRS; ischemia; cells

Since the discovery of ischemia-induced decreases in diffusion coefficients measured in brain tissue, diffusion-weighted (DW) MRI has been successfully used to diagnose and evaluate acute clinical stroke (1,2). The apparent diffusion coefficient (ADC) of tissue water drops significantly following cerebral ischemia, enabling easy identification of ischemic tissue in DW images. Although this observation has been clinically useful over the last several years, there is not a comprehensive understanding of the biophysical mechanisms underlying the reduction of tissue ADC. Many conditions could effectively slow down the movement of water in ischemic tissue and result in a measured drop in the ADC. These include: ischemia-induced cellular swelling, which results in an increase in the intracellular volume fraction (IVF) and increases in the tortuosity of the extracellular space; decreases in temperature; decreases in membrane permeability; and decreases in the intrinsic energy-

*Correspondence to: Theodore Trouard, Biomedical Engineering, 1657 E Helen Street, PO Box 210240, University of Arizona, Tucson, AZ 85721-0240. trouard@email.arizona.edu.

dependent motion of intracellular water (i.e., cytosolic streaming) (Ref. 3 and references therein). A number of theoretical models have been developed that attempt to take many relevant physiological parameters into account while modeling the results of DWMRI experiments, including: cell shape and size; unique intrinsic diffusion coefficients and T_2 relaxation times of the water in the intracellular and extracellular spaces; membrane permeability; and shape-dependent tortuosity factors of the extracellular space (4–9).

To effectively evaluate these models and deepen our understanding of how each of these parameters affect experimentally measured DWMRI results, it would be very useful to have experimental determination of as many of the modeling parameters as possible. In particular, the diffusion coefficient of water in the intracellular and extracellular space has been the focus of a significant amount of research. Because intracellular and extracellular water are typically not resolved spectroscopically, multiexponential analysis of signal decay curves from the total water signal has been used to assign diffusion properties of the intra- and extracellular spaces in cell cultures (10) and in living tissue (11,12). Contrast agents that differentially affect relaxation times in the intra- and extracellular spaces have also been used in conjunction with diffusion experiments to differentiate diffusion in the intra- and extracellular spaces (13–15). Finally, many surrogate markers of water diffusion have been investigated, including endogenous metabolites (16–18), ions (19,20), and exogenous biomolecules (21,22).

To allow more direct measurements of intracellular water properties, we have employed a novel three-dimensional (3D) hollow-fiber bioreactor (HFBR) perfused cell culture system that enables cells to be grown to high density in a homogeneous and controlled environment and be studied via MRI and MRS (23,24). The energetic status of cells can be noninvasively monitored via ^{31}P MRS, while water diffusion in the same cell culture can be measured via ^{1}H MRS and MRI. A unique and particularly useful feature of this HFBR system is that, with the infusion of a susceptibility contrast agent, MR signals from the intracellular and extracellular spaces become spectroscopically separated, allowing individual study of water in the intracellular space (25). In this communication, we report results from experimentally-induced ischemia in a HFBR culture of rat glioma cells. Diffusion properties of the intracellular water were measured before and after the onset of permanent ischemia and compared to the loss of energetic metabolites and cellular swelling, all obtained via MR techniques in the same cell culture. To our knowledge, this is the first report of the direct measurement of intracellular water diffusion in response to ischemia that has been made in living mammalian cells.

MATERIALS AND METHODS

HFBR

The HFBR system has been described in detail elsewhere (25). Briefly, the HFBR used in this study consists of a cylindrical polycarbonate casing (80-mm length, 27-mm outer diameter) containing approximately 450 microporous hollow fibers (700-μm outer diameter, 100-μm wall thickness) with a pore size of 0.2 μm. Cells are grown in the extrafiber spaces and are supplied with nutrients by continuous flowing of oxygenated media (O_2 = 60%, CO_2 = 5%, and N_2 = 35%) through the lumen of the fibers at a flow rate of 150 ml/min. An

external standard, 100 mM dimethylmethylphosphonate (DMMP) solution, within a sealed capillary tube, was placed into a channel machined into the wall of the HFBR and used to quantitatively evaluate ^{31}P MRS.

Cell Culture

Rat glioma (C6) cells were obtained from American Type Culture collection and routinely cultured in Dulbecco's modified Eagle's medium (DMEM) supplemented with 10% fetal bovine serum (FBS). Approximately 4×10^8 C6 cells were infused into the extrafiber space at the beginning of the experiment through an inoculation port in the side of the HFBR casing. The average cell diameter of the C6 cells as measured in suspension was approximately 12 μm.

MRI and Spectroscopy

All experiments were carried out at 9.4 Tesla on a Bruker AVANCE spectrometer equipped with self-shielded orthogonal imaging gradients (maximum strength = 1000 mT/m and rise time = 150 μs). A 27-mm dual tuned (^{31}P/^{1}H) birdcage RF probe was used for excitation and reception in all experiments (Bruker, Karlsruhe, Germany). To monitor cell growth, fully relaxed ^{31}P spectra were obtained daily via a one-pulse sequence using a 30° pulse every 1 s, collecting 4096 points over a spectral width of 100 ppm (3600 averages, 60-min acquisition time). The spatial distribution of cells within the bioreactor was monitored by DWMRI using a standard DW spin-echo, as previously described (25). After approximately 250 h of growth, the extrafiber space was filled with cells as the culture reached confluence, as evidenced by maximization of the nucleoside triphosphates (NTP) signals and homogeneously minimal ADC values throughout the extrafiber space.

Experimental Ischemia

Prior to the induction of ischemia, a 5-mM Gd-DTPA (Magnevist®, Bayer HealthCare Pharmaceuticals Inc, NJ, USA) solution was added to the media to split the water resonance of the HFBR into three separate signals, corresponding to intracellular water (unshifted), intraluminal/extracellular water (shifted +185 Hz) and water within the fiber wall (shifted +135 Hz), as described (25). Preischemia ^{31}P MRS spectra were recorded (4096 points, spectral width = 5000 Hz, TR = 500 ms, flip angle = 30°, and acquisition time = 2 min) to determine baseline metabolite levels and culture pH. A single-average one-pulse ^{1}H MRS experiment (flip angle = 30°, spectral width = 5000 Hz) was carried out to determine preischemia IVF. ^{1}H DWMRS experiments were carried out using a Stejskal-Tanner pulsed gradient spin-echo (PGSE) sequence employing balanced gradient pulses with duration (δ) = 7 ms, and pulse separation (Δ) = 14, 20, and 25 ms. The diffusion gradient strengths were adjusted for each Δ value to produce 16 *b*-values ranging from 0 to 1000 s/mm^2. Other experimental parameters were TE = 30 ms, and TR = 2.5 s.

To induce ischemia, the pump supplying media to the reactor was shut off, and repetitive ^{31}P MRS and ^{1}H MRS acquisitions were initiated in the presence of Gd-DTPA to monitor energetic status and cell volume. ^{31}P MRS spectra were recorded every 2 min followed by a single, average, one-pulse ^{1}H MRS experiment. When NTP was depleted from the culture (NTP resonance reduced to the level of the ^{31}P spectral noise), ^{1}H DWMRS experiments

were initiated and interleaved into the experimental cycle. The total experimental time for the three-experiment sequence was approximately 10 min and these were carried out over the course of 8 h following the onset of ischemia. Culture temperature was monitored via a fiber optic temperature probe and maintained at 37 ± 0.5°C throughout the entire experiment by running heated water through the MRI gradient coils surrounding the HFBR.

Data Analysis

Energetic metabolite levels were determined by monitoring the intensity of the β-NTP peak (23). IVF was determined from ^{1}H spectra by fitting individual spectra to three Lorentzian peaks and dividing the intracellular peak area by the total area of the spectrum. The intracellular ADC (iADC) before and after ischemia was calculated by fitting the area of the peak corresponding to intracellular water to a single exponential decay over the range of $b = 0–1000$ s/mm^2. Although the diffusion in the intracellular space over a large range of *b*-values is nonmonoexponential (12,25), the data obtained over these low *b*-values is adequately fit by a single exponential decay.

RESULTS

A preischemia ^{31}P spectrum obtained from C6 cells at confluence is shown in Fig. 1a. Signals from NTP, inorganic phosphate (P_i), glycerophosphorylcholine (GPC), and phosphomonoesters (PMEs) can be easily identified and are labeled in the figure. The energetic profile has been shown to be remarkably stable during cell growth (23). The signal from P_i resonance is comprised of peaks from intracellular and extracellular P_i and indicates only small changes in pH throughout the bioreactor. The chemical shift of the P_i resonance can be used to calculate intracellular pH, pHi (26), and indicates an average, preischemia pH value of 7.2.

Preischemia ^{1}H spectra are shown in Fig. 1b and demonstrate the effect of the Gd-DTPA on the water signal in the HFBR. Prior to the infusion of Gd-DTPA, the ^{1}H spectrum of the C6 HFBR culture consists of a single resonance set 0 Hz. After the addition of 5 mM Gd-DTPA to the perfusing media, the spectrum is split into three separate peaks. The peak near 0 Hz comes primarily from water in the intracellular space. The signal at +185 Hz arises primarily from water inside the lumen of the fibers and the extrafiber/extracellular space and water within the porous fiber wall is shifted +135 Hz. Justification of these assignments involved relaxation and diffusion measurements and has been previously described (25). Exchange of water between the intracellular and extracellular spaces, while not sufficient to cause coalescence of the observed peaks, will tend to decrease their spectral separation and broaden their linewidths, i.e., decrease their measured T_2 relaxation times. Neglecting these effects, a cellular volume fraction of approximately 0.75 in the extrafiber space was calculated.

Representative ^{31}P spectra before and after ischemia are shown in Fig. 2. Within minutes after shutting of the pump supplying media to the HFBR, decreases in the β-NTP peak are noticeable, and by 60 min after the onset of ischemia the β-NTP peak is reduced to the level of the noise. There is also a shift of the intracellular P_i resonance to the right (downfield) with time, indicating a decrease in the intracellular pH of the culture.

Representative ^{1}H spectra before and after the onset of ischemia are shown in Fig. 3. Spectra were chosen that reflect major changes observed over time. Within the first hour of ischemia, the resonance corresponding to intracellular water decreased in linewidth, increased in intensity, and shifted to the right. The resonances corresponding extracellular water (intrafiber, fiber wall, and extracellular water) shifted toward the left and decreased in intensity. At 2 h after ischemia the extracellular resonance continued to shift to the left and broaden while the intracellular resonance continued to increase in intensity. By 270 min postischemia, the intracellular and extracellular peaks broadened and began to coalesce, with both peaks approximately at their preischemia chemical shifts. After 340 min of ischemia the intracellular resonance decreased in size while the extracellular peak increased and there was significant spectral overlap. At 470 min after ischemia, the extracellular resonance shifted to the right of its preischemia chemical shift and there was significant spectral overlap of the three resonances. Interestingly, there is a small but visible signal left at 0 Hz, the preischemia location of intracellular water

The decrease in the energetic metabolites and the calculated changes in pH and IVF are plotted vs. time after ischemia in Fig. 4a–c. Almost immediately after shutting off the pump supplying media to the HFBR, there is a decrease in the β-NTP level, indicating very little nutrient reserve in the HFBR culture. By approximately 60 min postischemia, the β-NTP is depleted and remained so for the remainder of the experiment. The pH of the HFBR culture, calculated from the P_i chemical shift, dropped upon induction of ischemia and within 26 min has reached an acidic value of 6.3 where it remained for the duration of the experiment. There was also an observed splitting of the P_i signal, assigned to the intracellular and extracellular spaces. IVF experienced little change for approximately 15 min after the onset of ischemia but increased rapidly over the next 20 min after which it leveled off. At approximately 75 min postischemia, the IVF began to decrease and, after approximately 200 min of ischemia, the spectra became problematic to fit as they coalesced and broadened.

The ADC of the iADC measured at three diffusion times before and after the onset of ischemia is plotted in Fig. 4d. Preischemia values of iADC were significantly lower than those measured in tissue and demonstrate a diffusion time (Δ) dependence (over the small range of Δ covered), which indicated effects of restriction of the intracellular water. Postischemia diffusion measurements were initiated when the β-NTP levels had effectively disappeared from the ^{31}P spectrum (approximately 60 min) and repeated every 10 min thereafter. At 60 min postischemia, there was a significant increase in the iADC for all diffusion times studied, followed by smaller increases over time and leveling off at approximately 200 min postischemia. It should be noted that fitting the ^{1}H spectra after this time point become problematic due to the spectral overlap and therefore iADC values were not available.

DISCUSSION

These HFBR cell culture experiments illuminate important issues regarding water diffusion in ischemic tissue. Following the cessation of oxygen and nutrient delivery to the HFBR cell culture, there was a rapid decrease in the intracellular energetic metabolites. The rate

at which the metabolites disappeared indicates that there was very little energy reserve within the cells and HFBR, likely due to the high cell density maintained in the culture prior to ischemia. Within the first hour after ischemia, the energetic metabolites disappeared, concurrent with a decrease in the pH of the culture and an increase in the IVF due to cell swelling. The cell swelling plateaued coincidentally with depletion of the high-energy metabolites. The width of the intracellular water resonance narrows for the first few hours of ischemia, indicating an increase in T_2 or T_2^* relaxation. This could be due to a decreased influence of the extracellular Gd-DTPA on intracellular water due to an increase in cell volume, or possibly to a decrease in the interactions of intracellular water with intracellular surfaces due to dilution of the intracellular space. The shift of the extracellular peaks to the left following ischemia indicates an increase in the bulk susceptibility effect of Gd-DTPA. As cells swell, the extracellular volume decreases and the effective concentration of Gd-DTPA increases in the extracellular space of the HFBR. This causes a greater susceptibility shift of the extracellular peaks. The intracellular water resonance does exactly the opposite, shifting toward the right as cells swell, indicating a decrease bulk susceptibility shift from its preischemia value.

Approximately 2.5 h after the onset of ischemia, the intracellular water resonance begins to decrease and broaden and the intracellular and extracellular peaks begin to coalesce (Fig. 3). This is consistent with the cell membranes becoming permeable to Gd-DTPA. As Gd-DTPA enters permeabilized cells, the water resonance within those cells will shift toward that of the extracellular space. This will result not only in a reduction of the intracellular water signal but also in an effective reduction in concentration of Gd-DTPA within the extracellular space and the newly permeabilized intracellular space. This, in turn, will reduce the susceptibility induced shift toward lower values and result in a shift of extracellular peaks to the right (see Fig. 3).

The most significant results of these experiments came from the measurement of iADC before and after ischemia. The value of iADC before ischemia ranged from 0.35 to 0.5 $\mu m^2/ms$ for diffusion times of 25 to 14 ms, respectively. The low value of iADC (compared to free water) and its dependence on diffusion time indicates restricted diffusion in the intracellular space. The hardware available did not allow us to investigate shorter diffusion times and thus it was not possible to determine the unrestricted diffusion coefficient of intracellular water. The iADC values measured here were in the range of ADCs measured in Artemia cysts (27) and are similar to the slow diffusion coefficients obtained from biexponential fitting of diffusion decay curves in brain (11,12). It should be noted, however, that the slow diffusion component in living tissue has not been directly associated with the intracellular space. The values we report here are higher than the iADC determined in human breast cancer cell suspensions (0.11 $\mu m^2/ms$) in the very first diffusion measurements carried out in cell cultures (10). However, a direct comparison is difficult because the previous experiments were carried out at room temperature, using much longer diffusion times (Δ = 150.5 ms), and iADC was calculated from fitting signal decay at much higher *b*-values. All of these differences would tend to reduce the measured diffusion. The iADC values measured here are somewhat lower than those calculated from experiments employing contrast agents to separate intracellular and extracellular spaces in rat brain

(15), where values of 0.69 μm^2/ms were reported (diffusion time = 74 ms). It should be noted, however, that these in vivo values were calculated from the decay of the total water signal (intracellular + extracellular) under the assumptions that: 1) there was no MR signal contribution from the extracellular space due to complete T_2 dephasing of the extracellular signal by the contrast agent infused into the brain; and 2) there was no exchange between intracellular and extracellular spaces during the diffusion experiment. Invalidity of either of these assumptions would tend to result in an overestimation of intracellular diffusion.

An increase in iADC after ischemia, but before permeabilization of the cells to Gd-DTPA, was observed at all three diffusion times studied and indicated increased translation mobility of water within the cells. This is consistent with a dilution of the intracellular space by increased water content due to a shift of water from the extracellular space to intracellular space, as observed independently via ^1H spectroscopy. There are many possible explanations for the increase in water diffusion within the cell after ischemia. Dilution of the intracellular milieu by increasing water content would tend to decrease intracellular viscosity and thereby increase the intrinsic motion of water. Breakdown of macromolecular structures inside the cell could also decrease the organization of water hydration layers within the cell. Both of these effects have been observed from electron spin resonance studies of the intracellular space in mammalian cells (28). Also, changes in intracellular sodium concentrations could cause alterations in the size and/or ordering of intracellular organelles and possibly reduce the effective size of intracellular barriers or restrictions. Because the iADC was measured only after the depletion of energetic metabolites, it is unknown if iADC changes can be detected immediately after induction of ischemia or if changes occur after the depletion of significant amount of energetic metabolites.

The observation of increased iADC following ischemia reported here is in contrast to previous experiments that measured pre- and postischemia diffusion of intracellular metabolites (16–18), intracellular ions (19,20), and other biomolecules (21,22). In each of these previous studies, a reduction in the apparent diffusion of the intracellular marker or ion was observed following ischemia. These observations were generally interpreted to result from a reduction in an energy-dependent movement of molecules or ions (cytoplasmic streaming) and it was inferred that the same might hold true for intracellular water (20–22). It was recognized, however, that the intracellular motion of metabolites, ions, and molecules within the cell might not be the same as intracellular water (20,22). The increase in iADC following ischemia measured in the current set of experiments argues against the presence of preischemia intracellular or cytosolic streaming in these cells in regard to water. If energy-dependent streaming of water existed before ischemia, it is unlikely that an increase in the iADC following a depletion of energetic metabolites would be observed.

It is important to note that the observed increase in the iADC of water is not inconsistent with a decrease in the total water ADC typically observed in tissue following ischemia. The ADC observed in brain tissue decreases by 30% to 60% following acute ischemia. Models that predict ADCs from simple geometries demonstrate that cell swelling, i.e., shifts of water from the extracellular to the intracellular space and increasing tortuosity of the extracellular space, plays a significant role in the observed decreases in ADC, which is not removed by increases in iADC such as those observed here (4,5,8,9). Unfortunately, the geometry

of the HFBR and the addition of Gd-DTPA prevented the accurate determination of ADC from the extracellular space following ischemia. Nearly half of the space inside the HFBR is within the hollow fiber lumen and wall. The extracellular space, then, includes space that is not adjacent to cells. While contribution of signal from this space can be suppressed while the HFBR is flowing, it is not easily suppressed after the pump is shut off. The ADC of the total water signal measured within a flowing HFBR, with signal from within the fibers suppressed, was measured to be approximately 0.9 $\mu m^2/ms$, similar to that measured in tissue.

Although the data presented here is limited in terms of the number and range of diffusion times studied, the dependence of signal decay on diffusion time indicates the presence of restriction and can be fit to known mathematical models of intracellular diffusion to estimate parameters such as restriction lengths, i.e., cell sizes, and intrinsic diffusion coefficients. By neglecting exchange between the extracellular and intracellular compartments, these models can be employed to fit signal decay originating from the intracellular space of restricted geometries. Such models have been presented by Tanner and Stejskal (30) for parallel membranes assuming a short gradient pulse approximation, Balinov et al. (31) for parallel membranes using a Gaussian phase distribution approximation, and Murday and Cotts (32) for spherical geometries assuming a Gaussian phase distribution approximation. By simultaneously fitting the intracellular signal decay vs. *b*-value obtained at 14, 20, and 25 ms diffusion times, these models predict the intrinsic diffusion coefficients and restriction lengths reported in Table 1. Minimum error solutions are obtained from the preischemia data with cell dimensions between 8.2 and 13.4 μm and intrinsic (unrestricted) intracellular diffusion coefficients between 0.87 and 1.08 $\mu m^2/ms$. The cell dimensions are in the range of those measured in culture flasks using conventional microscopy, i.e., 12 μm, and intrinsic diffusion coefficients are, as expected, higher than the iADC calculated from single exponential fits. Minimum error fits to the postischemia data predicted and increase in intrinsic intracellular diffusion between 73% and 80%. However, these fits predict a decrease in cell size between 7% and 20%, which is in conflict with the experimental ^1H spectra. Table 1 also contains parameters from fits to postischemia data, where the cell size is prescribed to increase relative to preischemia values to match the change in IVF measured in ^1H spectra. In this case, each of the models still predict an increase in the intrinsic diffusion coefficient of water following ischemia, but the increase is less than that predicted from the minimum error solutions, i.e., between 9% and 15%. These results, while interesting, should be taken with caution as these simple models do not consider exchange with the extracellular space and only a narrow range of diffusion times were investigated. Future studies will investigate diffusion properties over a much wider range of diffusion times so that more realistic models can be used in the analysis.

Finally, it is important to note that the experiments described in this communication were carried out in C6 cell cultures and the generality of these results to other cell cultures, to neurons, or to tissue has not been established. C6 cells were employed in these experiments because they are a well-characterized cell line that retain many glial-specific properties (24–26,29) and will fill the extrafiber space in the HFBR to tissue-like cell densities. This is an important feature for investigating water motion within and between cells. However, being cancer cells, C6 cells may react differently to ischemia and hypoxia compared to

noncancerous cells or normal tissue. Cancer cells often have selective advantage to living in environments of low pH and hypoxia compared to normal cells, and their response to changes in the environment may also be different. Also, the preischemia internal movement of water within the C6 cell might be different than the movement in other types of cells.

CONCLUSIONS

The HFBR system is a unique and useful tool with which to study the diffusion properties of water in model cell cultures. With the inclusion of a common contrast agent, signal from water and intracellular spaces can be studied individually. The energetic status, pH, cell volume, and water diffusion can be monitored in the same cell cultures in conjunction with physiological challenges such as ischemia. Using the HFBR, diffusion properties of intracellular water before and after the onset of complete ischemia have been directly measured. Following ischemia, after energetic metabolites were depleted and cells were swollen, the ADC of intracellular water increased from its preischemia value. This is consistent with a dilution of the intracellular space and decrease in the density of intracellular barriers. This observation argues against the presence of energy-dependent intracellular streaming of water. The generality of this result will be assessed in future experiments on other cell lines and experimental conditions.

Acknowledgments

Grant sponsor: National Institutes of Health (NIH); Grant numbers: GM57270, CA88285.

REFERENCES

1. Moseley M, Cohen Y, Mintorovitch J, Chileuitt L, Shimizu H, Kucharczyk J, Wendland M, Weinstein PR. Early detection of regional cerebral ischemia in cats: comparison of diffusion- and T2-weighted MRI and spectroscopy. Magn Reson Med 1990;14:330–346. [PubMed: 2345513]
2. Warach S, Chien D, Li W, Ronthal M, Edelman RR. Fast magnetic resonance diffusion-weighted imaging of acute human stroke.Neurol 1992;42:1717–1723. [Erratum appears in Neurology 1992;42:2192]
3. Norris DG. The effects of microscopic tissue parameters on the diffusion weighted magnetic resonance imaging experiment. NMR Biomed 2001;14:77–93. [PubMed: 11320535]
4. Szafer A, Zhong J, Gore JC. Theoretical model for water diffusion in tissues. Magn Reson Med 1995;33:697–712. [PubMed: 7596275]
5. Latour LL, Svoboda K, Mitra PP, Sotak CH. Time-dependent diffusion of water in a biological model system. Proc Natl Acad Sci USA 1994; 91:1229–1233. [PubMed: 8108392]
6. Stanisz G, Szafer A, Wright G, Henkelman R. An analytical model of restricted diffusion in bovine optic nerve. Magn Reson Med 1997;37: 103–111. [PubMed: 8978638]
7. Pfeuffer J, Flogel U, Dreher W, Leibfritz D. Restricted diffusion and exchange of intracellular water: theoretical modelling and diffusion time dependence of ^{1}H NMR measurements on perfused glial cells. NMR Biomed 1998;11:19–31. [PubMed: 9608585]
8. Stanisz GJ. Diffusion MR in biological systems: tissue compartments and exchange. Isr J Chem 2003;43:33–44.
9. Vestergaard-Poulsen P, Hansen B, Ostergard L, Jakobsen R. Microstructural changes in ischemic cortical gray matter predicted by a model of diffusion-weighted MRI. J Magn Reson Imag 2007;26:529–540.

10. van Zijl PCM, Moonen CT, Faustino P, Pekar J, Kaplan O, Cohen JS. Complete separation of intracellular and extracellular information in NMR spectra of perfused cells by diffusion-weighted spectroscopy. Proc Natl Acad Sci USA 1991;88:3228–3232. [PubMed: 2014244]
11. Niendorf T, Dijkhuizen RM, Norris DG, van Lookeren Campagne M, Nicolay K. Biexponential diffusion attenuation in various states of brain tissue: implications for diffusion-weighted imaging. Magn Reson Med 1996;36:847–857. [PubMed: 8946350]
12. Mulkern RV, Gudbjartsson H, Westin CF, Zengingonul HP, Gartner W, Guttmann CR, Robertson RL, Kyriakos W, Schwartz R, Holtzman D, Jolesz FA, Maier SE. Multi-component apparent diffusion coefficients in human brain. NMR Biomed 1999;12:51–62. [PubMed: 10195330]
13. Stanisz GJ, Li JG, Wright GA, Henkelman RM. Water dynamics in human blood via combined measurements of T2 relaxation and diffusion in the presence of gadolinium. Magn Reson Med 1998;39:223–233. [PubMed: 9469705]
14. Li JG, Stanisz GJ, Henkelman RM. Integrated analysis of diffusion and relaxation of water in blood. Magn Reson Med 1998;40:79–88. [PubMed: 9660557]
15. Silva MD, Omae T, Helmer KG, Li F, Fisher M, Sotak CH. Separating changes in the intra- and extracellular water apparent diffusion coefficient following focal cerebral ischemia in the rat brain. Magn Reson Med 2002;48:826–837. [PubMed: 12417997]
16. van der Toorn A, Verheul HB, Berkelbach van der Sprenkel JW, Tulleken CA, Nicolay K. Changes in metabolites and tissue water status after focal ischemia in cat brain assessed with localized proton MR spectroscopy. Magn Reson Med 1994;32:685–691. [PubMed: 7869889]
17. Wick M, Nagatomo Y, Prielmeier F, Frahm J. Alteration of intracellular metabolite diffusion in rat brain in vivo during ischemia and reperfusion. Stroke 1995;26:1930–1933; discussion 1934. [PubMed: 7570750]
18. van der Toorn A, Sykova E, Dijkhuizen RM, Vorisek I, Vargova L, Skobisova E, van Lookeren Campagne M, Reese T, Nicolay K. Dynamic changes in water ADC, energy metabolism, extracellular space volume, and tortuosity in neonatal rat brain during global ischemia. Magn Reson Med 1996;36:52–60. [PubMed: 8795020]
19. Neil JJ, Duong TQ, Ackerman JJ. Evaluation of intracellular diffusion in normal and globally-ischemic rat brain via 133Cs NMR. Magn Reson Med 1996;35:329–335. [PubMed: 8699944]
20. Goodman J, Neil JJ, Ackerman JJ. Biomedical applications of 133Cs NMR. NMR Biomed 2005;18:125–134. [PubMed: 15770620]
21. Duong TQ, Ackerman JJ, Ying HS, Neil JJ. Evaluation of extra- and intracellular apparent diffusion in normal and globally ischemic rat brain via 19F NMR. Magn Reson Med 1998;40:1–13. [PubMed: 9660547]
22. Duong TQ, Sehy JV, Yablonskiy DA, Snider BJ, Ackerman JJ, Neil JJ. Extracellular apparent diffusion in rat brain. Magn Reson Med 2001; 45:801–810. [PubMed: 11323806]
23. Gillies RJ, Galons JP, McGovern KA, Scherer PG, Lien YH, Job C, Ratcliff R, Chapa F, Cerdan S, Dale BE. Design and application of NMR-compatible bioreactor circuits for extended perfusion of high-density mammalian-cell cultures. NMR Biomed 1993;6:95–104. [PubMed: 8457432]
24. Galons JP, Job C, Gillies RJ. Increase of GPC levels on cultured-mammalian-cells during acidosis —a P-31 MR spectroscopy study using a continuous bioreactor system. Magn Reson Med 1995;33:422–426. [PubMed: 7760711]
25. Galons JP, Lope-Piedrafitta S, Divijak JL, Corum C, Gillies RJ, Trouard T. Uncovering cellular water in cultured cells. Magn Reson Med 2005; 54:79–86. [PubMed: 15968680]
26. Barry JA, McGovern KA, Lien YH, Ashmore B, Gillies RJ. Dimethyl methylphosphonate (DMMP): a ^{31}P nuclear magnetic resonance spectroscopic probe of intracellular volume in mammalian cell cultures. Biochemistry 1993;32:4665–4670. [PubMed: 8485143]
27. Seitz PK, Chang DC, Hazlewood CF, Rorschach HE, Clegg JS. The self-diffusion of water in Artemia cysts. Arch Biochem Biophys 1981; 210:517–524. [PubMed: 7305341]
28. Mastro AM, Babich MA, Taylor WD, Keith AD. Diffusion of a small molecule in the cytoplasm of mammalian cells. Proc Natl Acad Sci USA 1984;81:3414–3418. [PubMed: 6328515]
29. Kempski O, Zimmer M, Neu A, Rosen Fv, Jansen M, Baethmann A. Control of glial cell volume in anoxia. In vitro studies on ischemic cell swelling. Stroke 1987;18:623–628. [PubMed: 3590256]

30. Tanner JE, Stejskal EO. Restricted self-diffusion of protons in colloidal systems by the pulsed-gradient, spin-echo method. J Chem Phys 1968; 49:1768–1777.

31. Balinov B, Jönsson B, Linse P, Söderman O. The NMR self-diffusion method applied to restricted diffusion. Simulation of echo attenuation from molecules in spheres and between planes. J Magn Reson A 1993; 104:17–25.

32. Murday JS, Cotts RM. Self-diffusion coefficient of liquid lithium. J Chem Phys 1968:4938–4945.

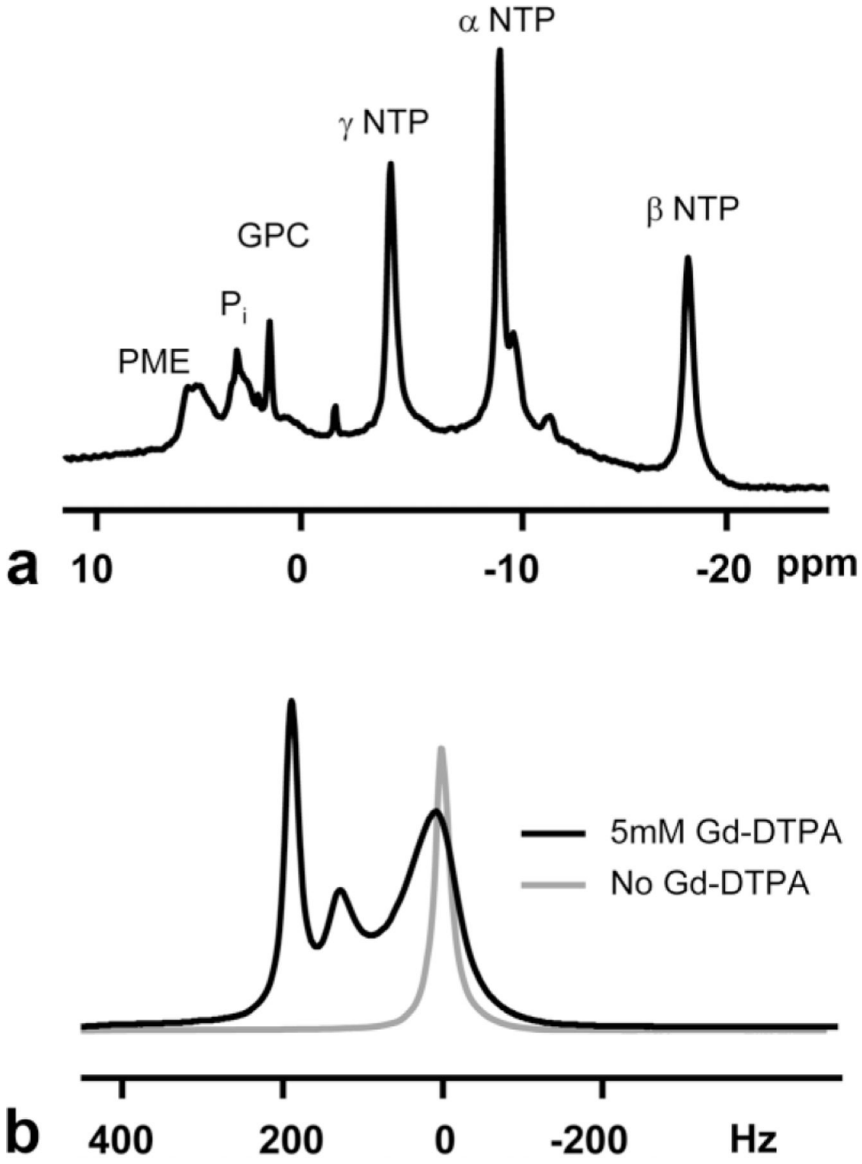

FIG. 1.

Preischemia ^{31}P (**a**) and ^{1}H (**b**) spectra of the HFBR C6 cell culture. Spectra were obtained at approximately 250 h of growth after inoculation. Labels in the ^{31}P spectrum are: GPC, glycerophosphorylcholine; NTP, nucleoside triphosphates; P_i, inorganic phosphate; and PME, phosphomonoesters. The ^{1}H spectrum was obtained before (black line) and after (gray line) the infusion of 5 mM Gd-DTPA into the media, which results in a splitting between intracellular (0 Hz) and extracellular (+185, +135 Hz) water components. The ^{1}H spectrum obtained before Gd-DTPA was scaled down by a factor of eight for plotting.

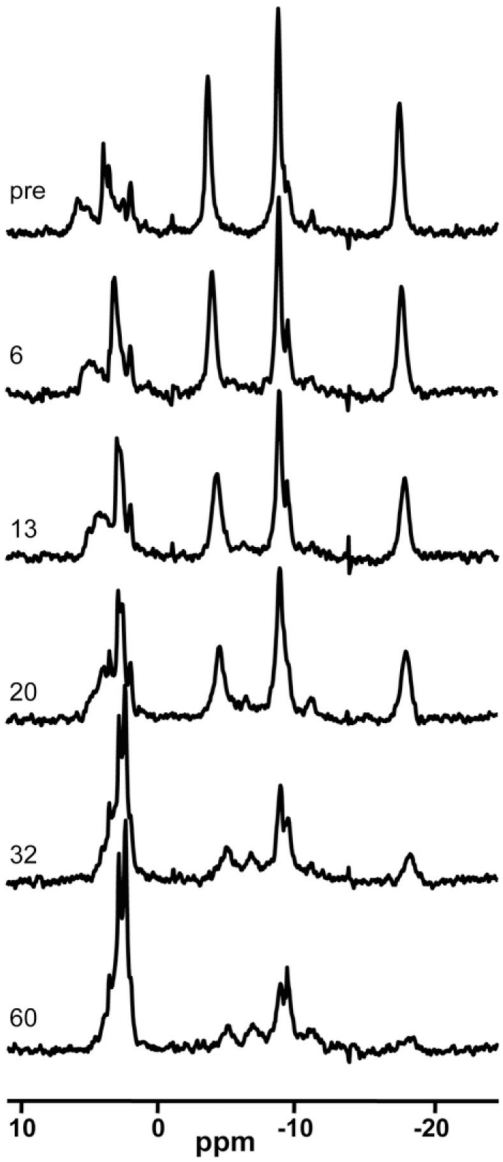

FIG. 2.

^{31}P MRS spectra of the HFBR C6 culture as a function of time after the onset of ischemia. Labels refer to the time after ischemia in minutes. Peak assignments can be found in Fig. 1.

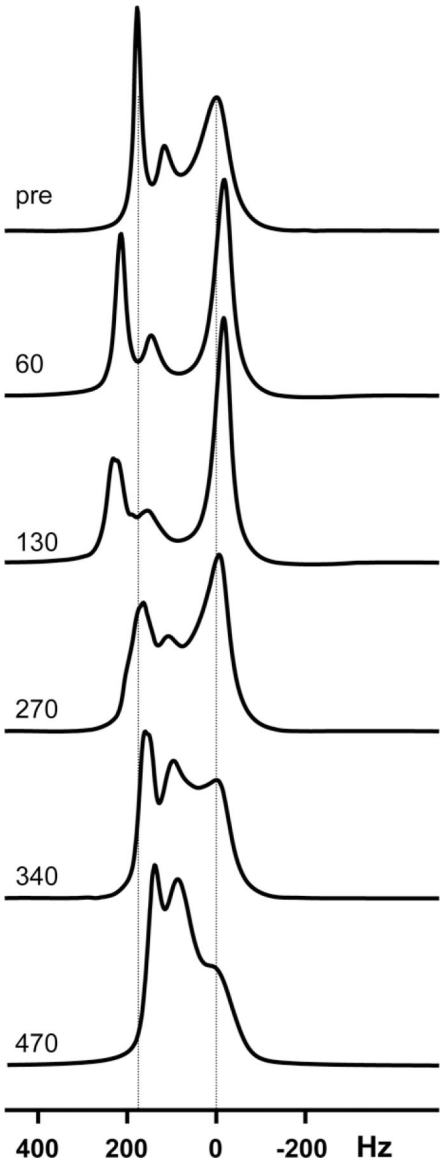

FIG. 3.

^{1}H MRS spectra of the HFBR C6 culture as a function of time after the onset of ischemia. Labels refer to the time after ischemia in minutes.

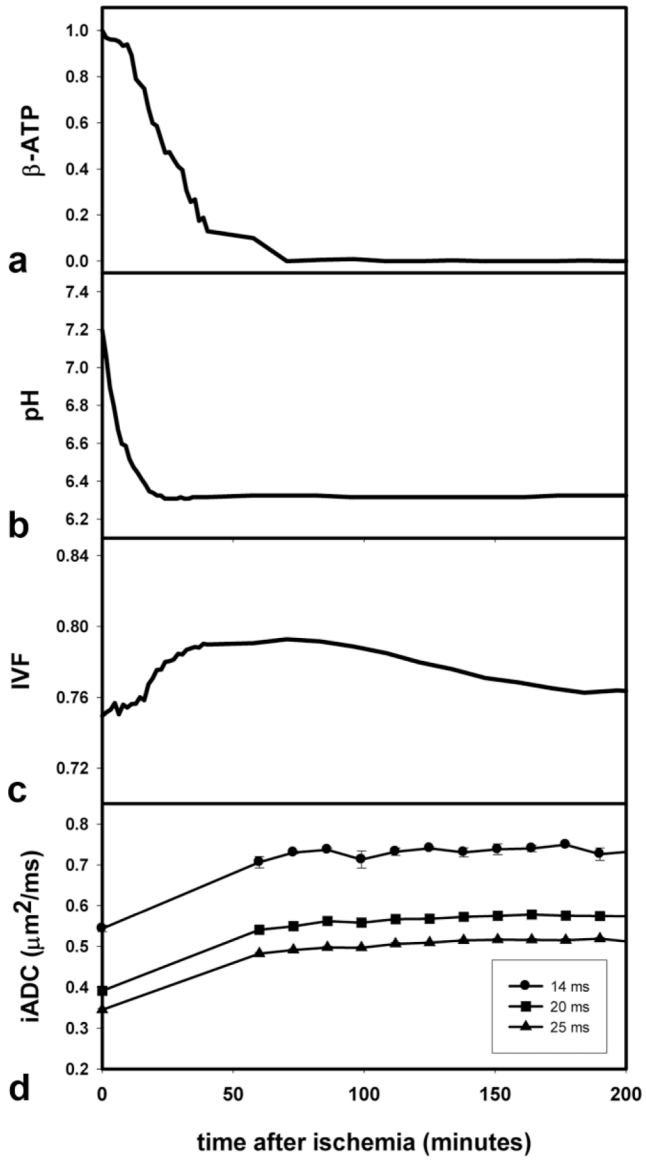

FIG. 4.

Calculated β-NTP levels (**a**), intracellular pH, pHi (**b**), IVF (**c**), and iADC (**d**) in the HFBR cell culture as a function of time after the onset of ischemia. β-NTP levels are normalized to preischemia values. Diffusion times (Δ) used in the three different iADC experiments are indicated in the insert of (d). A significant difference between the postischemia and preischemia iADC is observed at all diffusion times ($P < 0.005$, Student's paired *t*-test). Error bars in (d) represent error in the fit of data to a single exponential decay.

Table 1

Intrinsic Diffusion Coefficients (D_{int}) and Restriction Length (L_{res}) Predicted by Fitting Signal Decay Curves at Different Diffusion Times to Mathematical Models

	Preischemia		Postischemia		Postischemia[a]	
Model	**D_{int} (μm²/ms)**	**L_{cell} (μm)**	**D_{int} (μm²/ms)**	**L_{cell} (μm)**	**D_{int} (μm²/ms)**	**Lcell (μm)[a]**
Tanner and Stejskal (30)	0.87	13.70	1.56	10.94	0.95	13.94
Balinov et al. (31)	1.08	12.74	1.87	11.85	1.25	12.96
Murday and Cotts (32)	1.03	8.21	1.77	7.643	1.19	8.35

[a] In this fitting, L_{cell} was fixed based on spectroscopic cell volume fraction changes observed in the proton spectra relative to preischemia values.